Available online at www.sciencedirect.com
ScienceDirect
Journal of Environmental Sciences 2011, 23(4) 545–552
JOURNAL OF ENVIRONMENTAL SCIENCES
ISSN 1001-0742
CN 11-2629/X
www.jesc.ac.cn

Destruction of methylphosphonic acid in a supercritical water oxidation bench-scale double wall reactor

Bambang Veriansyah*, Eun-Seok Song, Jae-Duck Kim

Supercritical Fluid Research Laboratory, Korea Institute of Science and Technology (KIST), 39-1 Hawolgok-dong, Seoungbuk-gu, Seoul, 136-791, Korea. E-mail: vaveri@yahoo.com

Received 20 May 2010; revised 21 June 2010; accepted 30 June 2010

Abstract

The destruction of methylphosphonic acid (MPA), a final product by hydrolysis/neutralization of organophosphorus agents such as sarin and VX (O-ethyl S-[2-(diisopropylamino)ethyl] methylphosphonothionate), was investigated in a a bench-scale, continuous concentric vertical double wall reactor under supercritical water oxidation condition. The experiments were conducted at a temperature range of 450–600°C and a fixed pressure of 25 MPa. Hydrogen peroxide was used as an oxidant. The destruction efficiency (DE) was monitored by analyzing total organic carbon (TOC) and MPA concentrations using ion chromatography on the liquid effluent samples. The results showed that the DE of MPA up to 99.999% was achieved at a reaction temperature of 600°C, oxygen concentration of 113% storichiometric requirement, and reactor residence time of 8 sec. On the basis of the data derived from experiments, a global kinetic rate equation for the DE of MPA and DE of TOC were developed by nonlinear regression analysis. The model predictions agreed well with the experimental data.

Key words: supercritical water oxidation; destruction efficiency; methylphosphonic acid; reaction kinetic; nonlinear regression

DOI: 10.1016/S1001-0742(10)60446-9

Citation: Veriansyah B, Song E S, Kim J D, 2011. Destruction of methylphosphonic acid in a supercritical water oxidation bench-scale double wall reactor. Journal of Environmental Sciences, 23(4): 545–552

Introduction

Supercritical water oxidation (SCWO) provides a potential alternative for processing hazardous military waste without the concomitant production of noxious by-products, as might be experienced with combustion-based technologies (Veriansyah and Kim, 2007). SCWO uses supercritical water (T_c = 374°C and P_c = 22.1 MPa) as a reaction medium and exploits the unique solvating properties to provide enhanced solubility of organic reaction and permanent gases. SCWO is being applied in many pilot plants and a few commercial scale plants have been successfully demonstrated for complete destruction or organic waste efficiently. Despite the high potential of the SCWO process, the significant corrosion of reaction vessels and process equipment in SCWO process due to acidic byproduct has been obstacles for the successful application of chemical warfare agents (CWAs) destruction by SCWO process (Kritzer, 2004; Mitton et al., 2000; Veriansyah et al., 2005a, 2006a, 2007). Recently, we reported a newly designed bench-scale reactor to treat high-risk waste resulting from munitions demilitarization (Veriansyah et al., 2007, 2009). The performances of this reactor were investigated with three different kinds of CWAs simulants, including OPA (a mixture of isopropyl amine and isopropyl alcohol), thiodiglycol and a mixture of thiodiglycol and hydrochloric acid. High destruction rates based on total organic carbon (TOC) were achieved and no corrosion was noticed in the reactor after a cumulative operation more than 250 hr.

The present study examines the SCWO of methylphosphonic acid (MPA, $PO(OH)_2CH_3$) in our bench-scale reactor. MPA is a refractory hydrolysis product of organophosphorus CWAs, such as sarin and VX (O-ethyl S-[2-(diisopropylamino)ethyl] methylphosphonothionate), and is very resistant to hydrolysis, photolysis, and thermal decomposition (Munro et al., 1999). Information about the kinetics of MPA is essential for the design and optimization for complete destruction of organophosphorus CWAs. There have been previous experimental studies of MPA oxidation kinetics in supercritical water (SCW) based on destruction efficiency (DE) of MPA (Bianchetta et al., 1999; Sullivan and Tester, 2004). However, there are no references about MPA oxidation in the bench-scale reactor based on DE of MPA or DE of TOC. Bianchetta et al. (1999) used MPA as a rate-limiting model compound for VX/NaOH hydrolysate and used initial rate technique to determine reaction rate. The experiments were conducted using a laboratory scale continuous-flow

* Corresponding author. E-mail: vaveri@yahoo.com

reactor system and the study focused on measuring rates at high conversion (> 90%) to represent more practical treatment application. Conversions of greater than 99% were measured at 550°C, 27.6 MPa, 200% stoichiometric oxygen and residence times less than 20 sec. Sullivan and Tester (2004) conducted experiments to characterize the oxidation kinetics of MPA in SCW at moderate conversions in a laboratory plug flow reactor system. They reported that minimal conversion (< 30%) was measured at temperature < 503°C and residence time of 10 sec, whereas almost complete conversion (approximately 99%) was measure at temperature 571°C and residence time of 7 sec at stoichiometric conditions and pressure of 24.6 MPa.

The goals of this study are to determine the optimum operation conditions to achieve high DE of > 99.99% for MPA in our bench-scale SCWO reactor and to characterize the oxidation kinetics based on DE of MPA and DE of TOC. This study will contribute to the oxidation kinetic database for destruction of organophosphorus CWAs in the larger-scale destruction.

1 Materials and methods

1.1 Experimental apparatus

The experiments were conducted in a bench-scale, continuous-flow SCWO reactor system. A schematic diagram of the system including the SCWO reactor is shown in Fig. 1. The experimental setup, the reactor design, and the computational fluid dynamics (CFD) simulations of reactor system were described in previous publications (Song et al., 2006; Veriansyah et al., 2007).

The reactor (R) consists of a concentric vertical double wall. The external vessel with an inside diameter (I.D.) of 52 mm, an outer diameter (O.D.) of 102 mm, and an internal volume of 1274.74 cm^3 is made of Hastelloy C-276. The external vessel contains a reaction chamber limited by a non-porous wall which was constructed by a 590 mm length, 22 mm I.D. and 25.4 mm O.D. titanium grade 2 tubing. An annular gap is created between the external vessel and the reaction chamber. The inner tube confines the reacting medium inside the tubular space; thus, the Hastelloy C-276 vessel has no contact with the aggressive solutions generally treated by SCWO.

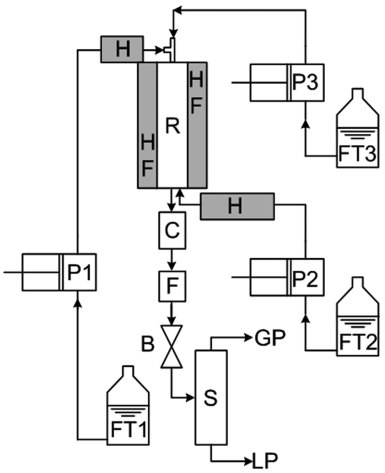

Fig. 1 Schematic diagram of supercritical water oxidation bench-scale double wall reactor. B: back-pressure regulator; C: condenser; F: metal filter; H: deionized water/oxidant preheater line; R: double wall reactor; S: gas-liquid separator; P1: high pressure pump for oxidant solution; P2: high pressure pump for deionized water; P3: high pressure pump for organic solution; FT1: feed tank for oxidant solution; FT2: feed tank for deionized water; FT3: feed tank for organic solution; HF: heat furnace; LP: liquid product; GP: gaseous product.

The distilled water, generally under supercritical condition around 25 MPa and 400°C, is introduced in the annular gap by its lower part, and it heated up to reaction temperature. In the top of annular gap, its direction is reversed entering the reaction chamber, and then, it flow downward, mixing with the waste and oxidant solution that enters into the reactor by the inlet dip pipe at the upper part. The products leave the reactor by its lower part. As the inner and outer flows are at the same pressure, no pressure constrains have to be considered.

Oxidant solution, waste solution, and distilled water were pumped separated into the reaction system using high-pressure pumps (P1, P2, or P3). The oxidant solution was preheated in 6 m of 3.175 mm O.D. coiled stainless steel (SS316) tubing by a cast heater (H) prior to its reactor input. The waste solution was injected directly into the reactor by the inlet dip pipe without being preheated, to avoid degradation of the waste. The distilled water was preheated in 12 m of 3.175 mm O.D. coiled SS316 tubing by a cast heater (H) prior to its reactor input.

The products of the reaction were cooled in a cooling unit (C) after leaving the reactor and, afterward, it were filtered to separate the solid particles through a 0.5 μm in-line metal filter (F) and finally depressurized to ambient condition by a back-pressure regulator (B, model 26-1721-24, Tescom Co., USA). After the product exited the regulator, it flashed to atmospheric pressure and the two-phase mixture was separated into two streams by gas-liquid separator (S). The gas flow rate was measured using a wet gas meter, while the liquid flow rate was measured by recording the time required to fill a volumetric flask. The gaseous effluent was injected into the two gas chromatographs while the liquid effluent samples were collected in a glass sample vials and analyzed using a TOC analyzer and an ion chromatography (IC).

1.2 Materials and analytical methods

Methylphosphonic acid ($PO(OH)_2CH_3$, purity of 98%) was purchased from Sigma-Aldrich, Co. (USA). Hydrogen peroxide (H_2O_2, 35%, *W*/*V*) as the oxygen source was obtained from Junsei Chemical Company (Japan). Distilled and deionized water was prepared using a Milli-Q, ultrapure water purification system with a 0.22-μm filter. All of the standard solutions for calibration and identification in liquid analytical methods were prepared using high-purity chemical (ACS grade, Sigma-Aldrich, Co., USA).

Gas samples were analyzed online using two Hewlett-Packard model 5890 Series II gas chromatographs (GC) with a thermal conductivity detector (TCD) and helium as the carrier gas, with detection limits ranging from 0.1 vol.% to 0.5 vol.%. The TOC concentration of the

MPA solution and the liquid-phase reactor effluent were analyzed using a TOC analyzer (TOC-VCSH, Shimadzu, Japan), with a detection limit of 0.01 mg/L. The concentration of MPA and phosphoric acid ion was determined by an ion chromatography (IC, model DX-100, Dionex, USA) equipped with an anion column (model IonPac AS14, Dionex, USA) and an anion self-regenerating suppressor (model ASRS-UltraII, Dionex, USA), with a detection limit of 0.02 mg/L. Details on GC, TOC analyzer and IC were described in the previous article (Veriansyah et al., 2005a).

1.3 Calculations

The effects of temperature, residence time, initial concentration of MPA, and oxidant concentration were studied.

1.3.1 Residence time calculation

The residence time (t) is calculating using the following Eq. (1):

$$t = \frac{V_R}{M_{total}} \times \rho(P, T) \tag{1}$$

where, V_R is the reactor volume, $\rho(P, T)$ is the density of fluid at reaction pressure and temperature, and M_{total} is the total feed mass flow rate including both the wastewater mixture and the oxidant fed into the system. The density of the fluid is taken from steam tables for pure water (Wagner and Pruβ, 2002) since the investigations performed with dilute solutions of MPA in the water and no data were available for density of water-MPA-oxygen mixtures at supercritical condition.

1.3.2 Initial concentration of MPA

The initial concentration of MPA at reaction condition was calculated from the measured feed stock concentrations and flow rates of the feed streams with the process condition, assuming that the fluid has the density of water (Wagner and Pruβ, 2002). For initial concentration of MPA (N_{MPA}, mol/L):

$$N_{MPA} = C_{MPA} \times \frac{M_{MPA}}{M_{total}} \times \rho(P, T) \tag{2}$$

where, C_{MPA} (mol/L) is MPA concentration in the feed stock, M_{MPA} (g/min) is MPA feed flow rate to reactor, and M_{total} (g/min) is the total feed mass flow rate including the water, the wastewater mixture, and the oxidant fed into the system.

1.3.3 Destruction efficient

The destruction efficient (DE) of MPA was expressed in terms of MPA and TOC conversion, following Eqs. (3) and (4):

$$DE_{MPA} = \frac{C_{MPAi} - C_{MPAo}}{C_{MPAi}} \times 100\% \tag{3}$$

$$DE_{TOC} = \frac{C_{TOCi} - C_{TOCo}}{C_{TOCi}} \times 100\% \tag{4}$$

where, C_{MPAi} and C_{MPAf} are the MPA concentration at the reactor inlet and outlet, whereas, C_{TOCi} and C_{TOCf} are the TOC concentration at the reactor inlet and outlet.

2 Results and discussion

A total of fifty SCWO experiments were conducted at different reaction temperatures (450–600°C), residence time (4.3–9.2 sec), and initial concentrations of MPA (4.4–17.0 mmol/L) and oxygen (113%–27% of O_2 stoichiometric requirement) at a fixed pressure of 25 MPA in the bench-scale double wall reactor system. A summary of each experimental condition and the measured conversions are shown in Table 1. A stoichiometric level of oxygen was determined using the assumption of the complete oxidation of MPA:

$$CH_5O_3P + 2O_2 \longrightarrow H_3PO_4 + 2H_2O + CO_2 \tag{5}$$

The reaction products include gaseous and liquid components. The gas analysis indicated the presence of CH_4, CO, CO_2 and O_2. A mass balance for both carbon and phosphor species were conducted for all experiments, based on the measured inlet concentration and outlet product. As for the carbon balance, the incoming carbon was based on carbon in the feed MPA, and the outgoing carbon was the sum of the carbon in the liquid and gas effluents. The detectable carbon in the gas effluents were CH_4, CO and CO_2. Therefore, Henry's law was used to calculate the dissolved CH_4, CO and CO_2 concentration in the liquid effluent, based on the concentration in the off-gas (Gopalan, 1995). The carbon balances had an average value of 95.7% ± 4.1%, with a range of 84.5%–105.7%. In regard to elemental phosphor, its oxidation would yield phosphoric acid. Consequently, the amount of this acid in the output stream was measure. The phosphor balance based on the measure phosphor in the inlet and outlet reactor. The incoming phosphor was based on the phosphor in the feed of MPA, and the outgoing phosphor was based on the phosphor in the liquid. The phosphor balance had an average value of 96.9% ± 6.4%, with a range of 84.4%–109.8%.

The effects of temperature and residence time on TOC conversion were determined at three reaction temperatures (450, 500, and 550°C), 183% of oxygen excess and initial MPA concentration of 10.7 mmol/L. Figure 2 shows that the conversion of TOC and MPA increases with higher reaction temperature and longer residence time. TOC conversions were all over 88% whereas the MPA conversions were all over 94%. It should be emphasize that MPA conversions were always higher than TOC conversion in all cases since C_{TOCf} may include unreacted MPA or intermediated products. The carbon fraction of the intermediates, CH_4 and CO, and the final carbon containing product, CO_2, are plotted in Fig. 3 as a function of residence time at reaction temperature of 450 and 550°C . The carbon fraction for species (i) is defined as Eq. (6).

$$i = \frac{MC_i}{TMC} \times 100\,\% \tag{6}$$

where, MC_i is the moles of carbon in ith product, TMC is the total moles of carbon feed.

As shown in the Fig. 3, CO_2 was the major oxidation product of MPA while CO and CH_4 is a minor product.

Table 1 Summary of MPA oxidation experiments at 25 Mpa

Reaction temperature (°C)	Residence time (sec)	Initial MPA concentration (mmol/L)	Initial TOC concentration (mg/L)	O_2 excess (%)	DE of MPA (%)	DE of TOC (%)
450	5.5	4.4	62	183	91.791	83.534
450	5.5	8.2	114.5	183	94.024	87.124
450	5.5	10.2	143.1	183	94.691	88.695
450	5.5	10.7	149.7	279	96.933	92.398
450	5.5	10.7	149.7	180	96.31	91.666
450	5.5	10.7	149.7	113	94.702	88.131
450	5.5	16.3	227.8	183	94.914	89.785
450	5.6	10.7	149.7	183	94.617	88.695
450	7.6	10.7	149.7	183	96.31	91.666
450	8	8.1	113.3	113	91.023	83.09
450	8	10.7	149.7	113	94.702	88.131
450	8	13.5	188.9	113	96.273	91.47
450	8	17	237.8	113	97.355	94.905
450	8	17	237.8	183	97.633	94.795
450	9.2	10.7	149.7	183	97.377	93.169
500	4.8	10.7	149.7	183	98.84	93.756
500	5.5	4.4	62.1	183	98.173	92.251
500	5.5	8.1	113.3	183	98.513	94.912
500	5.5	10.6	147.7	183	98.84	95.154
500	5.5	10.7	149.7	277	99.321	97.602
500	5.5	10.7	149.7	185	99.275	96.116
500	5.5	10.7	149.7	113	98.483	94.23
500	5.5	16	224.1	183	98.999	96.71
500	6.2	10.7	149.7	183	99.275	96.116
500	7.9	10.7	149.7	183	99.492	96.922
500	8	8.1	113.3	113	96.564	88.722
500	8	10.7	149.7	113	98.483	94.23
500	8	13.5	188.9	113	99.166	96.012
500	8	17	237.8	113	99.552	97.435
500	8	17	237.8	183	99.693	97.432
550	4.3	10.7	149.7	183	99.85	98.209
550	5.5	4.5	62.5	183	99.556	97.862
550	5.5	8.1	113.9	183	99.786	98.176
550	5.5	10.3	144.8	183	99.85	98.409
550	5.5	10.7	149.7	272	99.999	99.259
550	5.5	10.7	149.7	180	99.998	98.245
550	5.5	10.7	149.7	115	99.708	97.76
550	5.5	15.9	222.3	183	99.891	98.68
550	5.5	10.7	149.7	183	99.99	98.245
550	6.9	10.7	149.7	183	99.994	98.687
550	8	8.1	113.3	113	99.378	96.35
550	8	10.7	149.7	113	99.905	97.76
550	8	13.5	188.9	113	99.981	98.526
550	8	17	237.8	113	99.992	98.768
550	8	17	237.8	183	99.999	99.326
600	8	8.1	113.3	113	99.985	97.7
600	8	10.7	149.7	113	99.95	98.014
600	8	13.5	188.9	113	99.989	98.053
600	8	17	237.8	113	99.999	98.828
600	8	17	237.8	183	99.999	99.371

Within these experimental ranges, CO is a reactive intermediate and its fraction decreases with higher temperature, while CH_4 is a refractory intermediate, as its fraction relatively stable with temperature. The fraction of CO_2 increased continually over the experimental temperature ranges to a maximum value of 94.3% at 550°C where the MPA conversion was 99.99%.

The influence of the MPA concentration on the MPA and TOC conversion was determined at three reaction temperatures (450, 500, and 550°C), 183% of oxygen excess and a residence times of 5.5 sec at a fixed pressure of 25 MPa. As can be seen in Fig. 4, increasing MPA concentration enhances the MPA and TOC conversions. This indicates that the global reaction order for MPA is greater than zero. For the carbon fraction, as shown in Fig. 5, the CO_2 carbon fraction increased as MPA concentration increased, while CO and CH_4 were slightly decreased.

The influence of the oxidant concentration on the MPA and TOC conversion at three reaction temperatures (450, 500, and 550°C) was determined and a residence times of 5.5 sec, an initial MPA concentration of 10.7 mmol/L and a fixed pressure of 25 MPa. Figure 6 shows that MPA and TOC conversion increases with higher oxygen concentration of the feed. This implies that the global reaction order for oxidant also greater than zero.

Figure 7 shows the carbon fraction as the function of oxidant concentration and reaction temperature. The CO carbon fraction was decreased whereas the CO_2 carbon

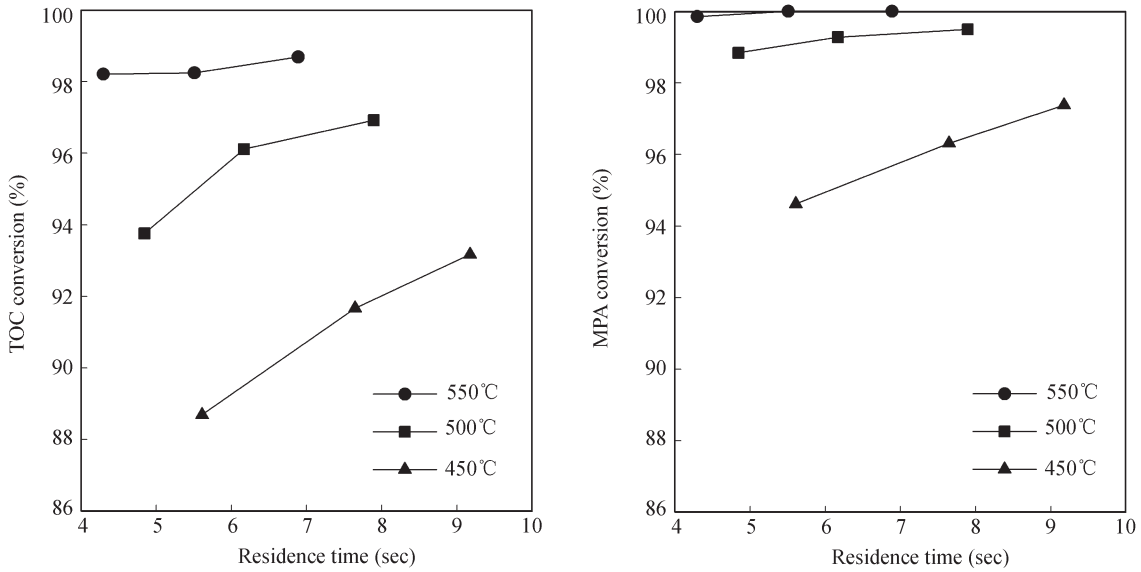

Fig. 2 Effect of temperature and residence time on TOC and MPA conversion.

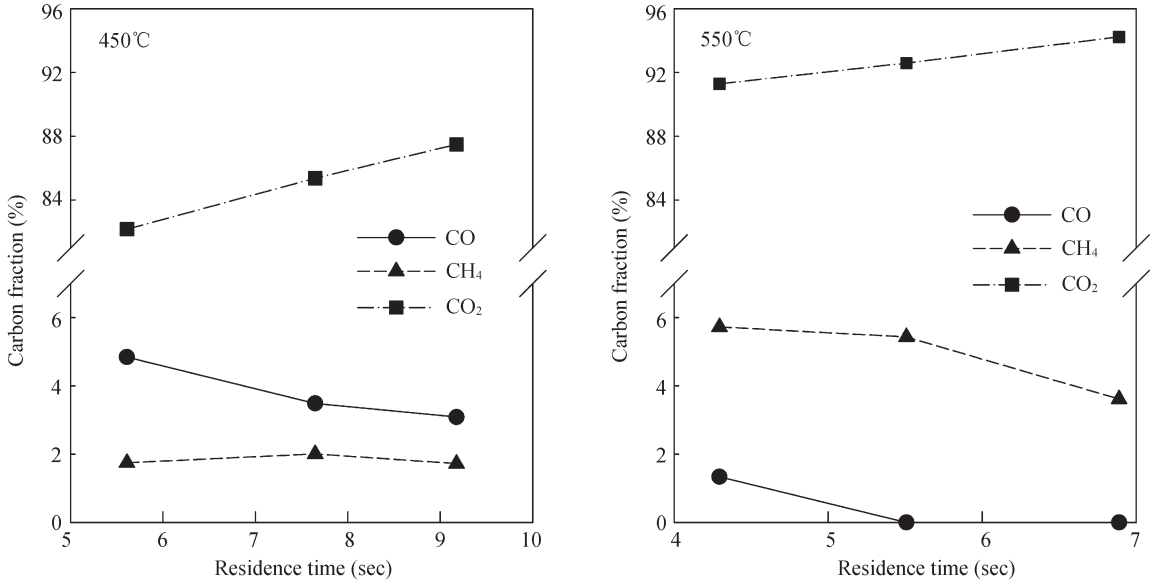

Fig. 3 Species carbon fraction of CH_4, CO and CO_2 in the reaction outlet stream, as a function of residence time at 450 and 550°C.

fraction was increased as the oxidant concentration and reaction temperature increased. Similar results were observed by Holgate et al. (1992) during their experiment on carbon monoxide oxidation in supercritical water. It was found that oxidation rate of CO to CO_2 has an oxygen and temperature dependence. As for the CH_4 carbon fraction, the fraction was decreased as the oxidant concentration increased. The CH_4 carbon fraction steadily increased when the reaction temperature below 550°C and then decreased as the reaction temperature increased further to 600°C. This implies that the oxidation of CH_4 is favorable at higher reaction temperature and oxidant concentration.

The global power-law rate reaction is used to predict the DE of MPA and DE of TOC in SCW. In this study, we assumed the global oxidation of MPA or TOC depends only on the temperature, the reactant concentration, and the oxidant concentration since the experimental data were measured at varying the reaction temperature, the reactant and the oxidant concentration at the fixed reaction pressure (Gopalan, 1995; Han et al, 2007; Veriansyah et al., 2005a, 2005b, 2006b). The water concentration was assumed to have no explicit effect on the reaction rate, as many reported SCWO kinetic studies (Anitescu and Tavlarides, 2000; Bianchetta et al., 1999; Gopalan, 1995; Han et al, 2007; Martino and Savage, 1999; Portela et al, 2001; Rice and Steeper, 1998; Schanzenbacher et al, 2002; Veriansyah et al., 2005a, 2005b, 2006b). Thereby, the global power-law reaction rate (r) can be expressed as :

$$r = -\frac{\mathrm{d}C_n}{\mathrm{d}t} = A\exp\left(-\frac{E_\mathrm{a}}{RT}\right)C_n^a C_{\mathrm{O}_2}^b \tag{7}$$

where, C_n (mmol/L) is the concentration of reactant; C_{O_2} (mmol/L) is the concentration of oxidant; t is the reaction time; a and b are the reaction orders of C_n and C_{O_2}; A and E_a are the pre-exponential factor and activation energy, respectively. A multivariable nonlinear least-squares

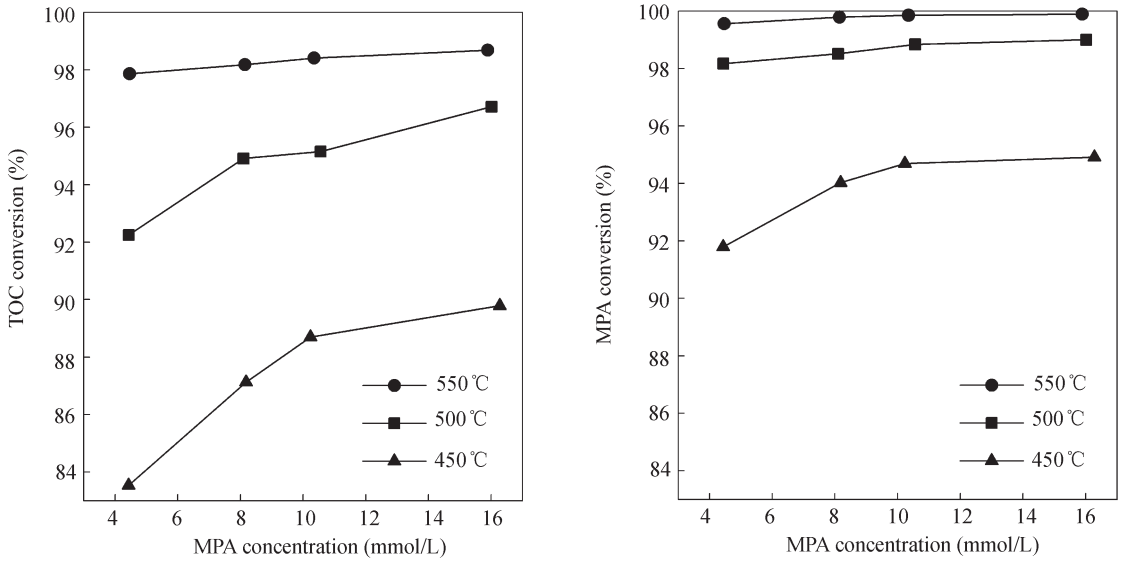

Fig. 4 Effect of MPA concentration on TOC and MPA conversion.

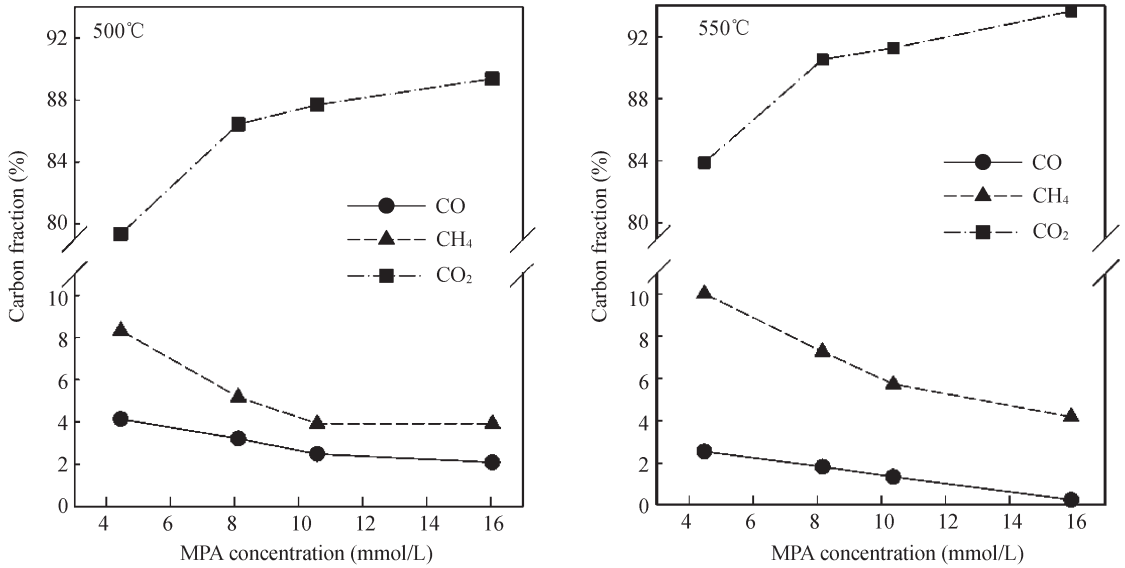

Fig. 5 Species carbon fraction of CH_4, CO and CO_2 in the reaction outlet stream, as a function of MPA concentration at 500 and 550°C.

technique was used to estimate the kinetic parameter A, the activation energy E_a, and the reaction order (Veriansyah et al., 2005a). Table 2 listes the kinetic parameter, the activation energy, and the reaction order based on MPA and TOC conversion.

Figure 8 shows a good comparison of the measured and predicted conversion for both TOC and MPA. The dashed line, which indicated a deviation ±4% (for TOC conversion) or ±3% (for MPA conversion) from the 45° line (perfect match), contains all data points. These models fit our experimental data very well.

Table 2 Kinetic data for MPA and TOC reaction rate

	a	b	A	E_a (J/mol)
TOC conversion	1.1720	0.1703	2.3931×10^5	66,768
MPA conversion	1.0771	0.1436	4.0066×10^5	73,367

3 Conclusions

An experimental study for the destruction of methylphosphonic acid (MPA), a final product by hydrolysis/neutralization of organophosphorus agents such as sarin and VX, in supercritical water oxidation (SCWO) was performed a bench-scale, continuous concentric vertical double wall reactor. Experimental data showed that MPA conversion were all > 90% whereas TOC conversion were all > 80% at temperature range of 450–600°C and a fixed pressure of 25 MPa. Especially, destruction efficiency of MPA up to 99.999% was achieved at a reaction temperature of 600°C, oxygen concentration of 113% storichiometric requirements, and reactor residence time of 8 sec. Conversion efficiency was significantly improved with temperature. Higher conversion were obtained at higher temperature, oxidant and MPA feed concentration. As the result of MPA

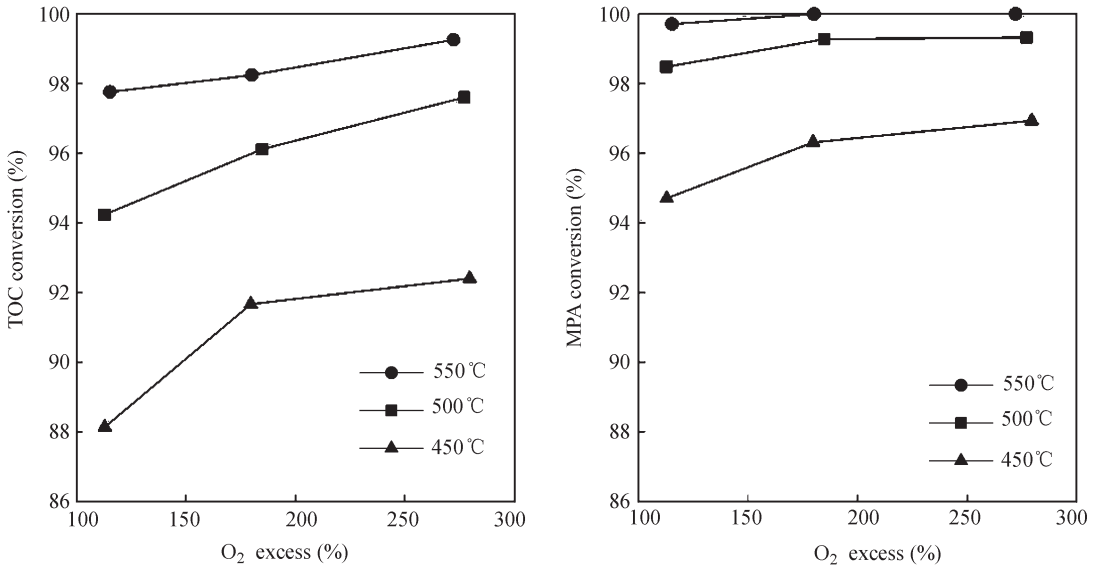

Fig. 6 Effect of oxidant concentration on TOC and MPA conversion.

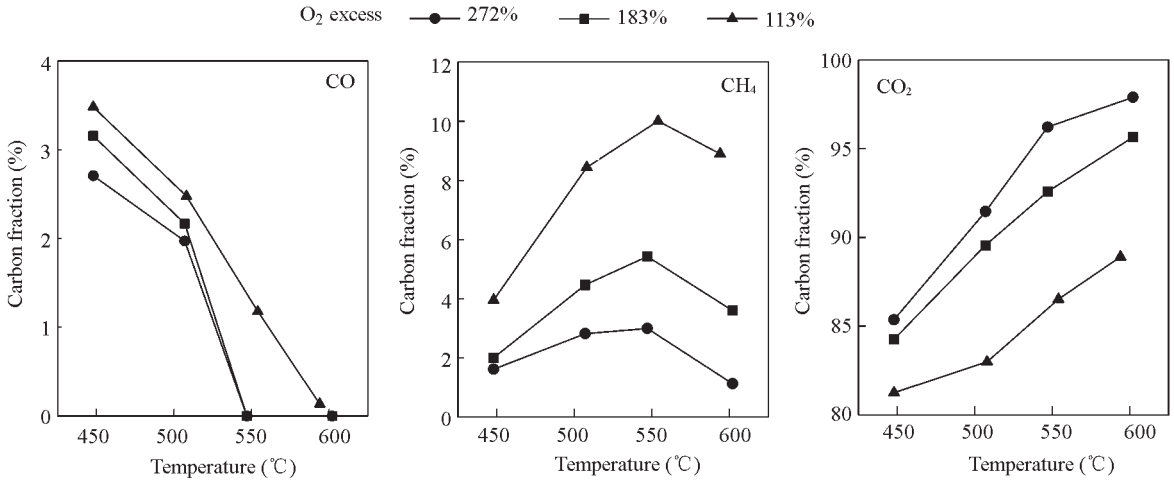

Fig. 7 Species carbon fraction of CH_4, CO and CO_2 in the reaction outlet stream, as a function of O_2 excess and temperature.

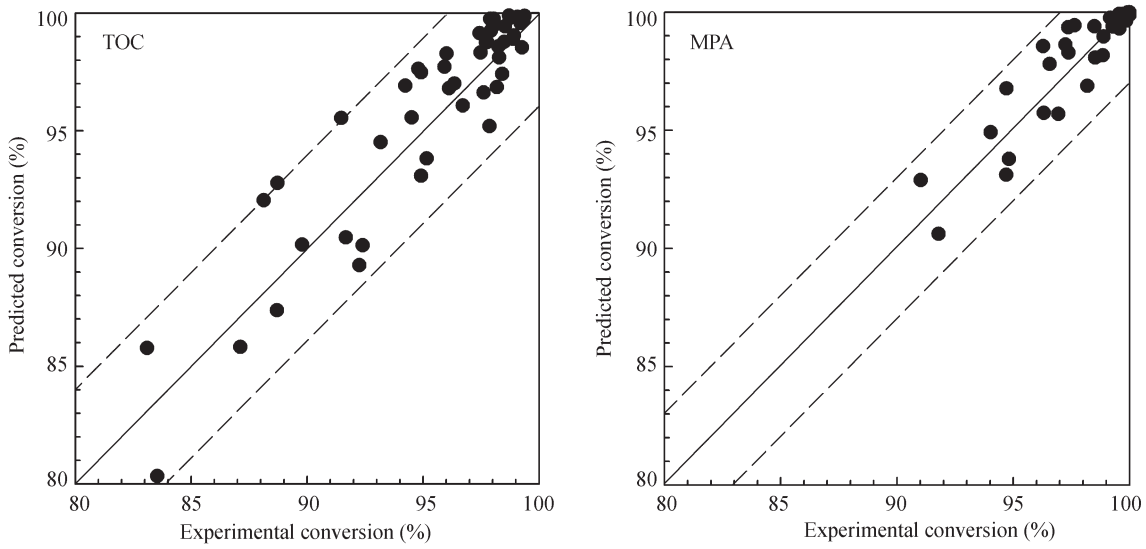

Fig. 8 Comparison of the predicted and experimental conversions.

oxidation, phosphoric acid was formed in the liquid-phase effluent while carbon monoxide, carbon dioxide and methane were observed in gas-phase effluent. The phosphor and carbon balances of this experiment had average values of (96.9 ± 6.4)% and (95.7 ± 4.1)%, respectively. By taking into account the dependence of reaction rate on the oxidant and MPA or TOC concentration, all experimental data were used to fit the reaction rate for MPA and TOC conversion in a nonlinear regression analysis, assuming a zero-order dependence on water concentration. The model predictions agree well with the experimental data.

Acknowledgments

This work was partially supported by Agency for Defense Development, Korea and Korea Institute of Science and Technology. We are grateful to Dr. Jong-Chol Lee from ADD for his valuable advice regarding MPA analysis procedure.

References

Anitescu G, Tavlarides L L, 2000. Oxidation of aroclor 1248 in supercritical water: A global kinetic study. *Industrial & Engineering Chemistry Research*, 39: 583–591.

Bianchetta S, Li L, Gloyna E F, 1999. Supercritical water oxidation of methylphosphonic acid. *Industrial & Engineering Chemistry Research*, 38: 2902–2910.

Gopalan, 1995. Phenol oxidation in supercritical water: from global kinetics to a detailed mechanistic model. Ph.D Thesis. The University of Michigan, Ann Arbor, MI.

Han S H, Veriansyah B, Kim J D, Lee J C, 2007. Pentachlorophenol oxidation rates in supercritical water. *Journal of Environmental Science and Health: Part A,* 42: 2105–2109.

Holgate H R, Webley P A, Tester J W, Helling R K, 1992. Carbon monoxide oxidation in supercritical water: The effects of heat transfer and the water-gas shift reaction on observed kinetics. *Energy Fuels*, 6: 586–597.

Kritzer P, 2004. Corrosion in high-temperature and supercritical water and aqueous solutions: A review. *Journal of Supercritical Fluids*, 29: 1–29.

Martino C J, Savage P E, 1999. Total organic carbon disappearance kinetics for the supercritical water oxidation of monosubstituted phenols. *Environmental Science and Technology*, 33: 1911–1915.

Mitton D B, Yoon J H, Cline J A, Kim H S, Eliaz N, Latanision R M, 2000. Corrosion behavior of nickel-based alloys in supercritical water oxidation systems. *Industrial & Engineering Chemistry Research*, 39: 4689–4696.

Munro N B, Talmage S S, Griffin G D, Waters L C, Watson A P, King J F et al., 1999. The sources, fate, and toxicity of chemical warfare agent degradation products. *Environmental Health Perspectives,* 107(12): 933–974.

Portela J R, Lopez J, Nebot E, de la Ossa E M, 2001. Elimination of cutting oil wastes promoted hydrothermal oxidation. *Journal of Hazardous Materials*, 88: 95–106.

Rice S F, Steeper R R, 1998. Oxidation rates of common organic compounds in supercritical water. *Journal of Hazardous Materials*, 59: 261–278.

Schanzenbacher J, Taylor J D, Tester J W, 2002. Ethanol oxidation and hydrolysis rates in supercritical water. *Journal of Supercritical Fluids*, 22: 139–147.

Song E S, Kim J D, Lee Y W, 2006. CFD simulations of the supercritical fluid process. In: Proceedings of 8th International Symposium of Supercritical Fluids (ISSF). Kyoto, Japan. 5–8 November. Paper PB-1-17.

Sullivan P A, Tester J W, 2004. Methylphosphonic acid oxidation kinetics in supercritical water. *American Institute of Chemical Engineers Journal*, 50(3): 673–683

Veriansyah B, Kim J D, 2007. Supercritical water oxidation for the destruction of toxic organic wastewater: A review. *Journal of Environmental Sciences,* 19(5): 513–522.

Veriansyah B, Kim J D, Lee J C, 2005a. Supercritical water oxidation of thiodiglycol. *Industrial & Engineering Chemistry Research*, 44: 9014–9019.

Veriansyah B, Park T J, Lim J S, Lee Y W, 2005b. Supercritical water oxidation of wastewater from LCD manufacturing process: kinetic and formation of chromium oxide nanoparticle. *Journal of Supercritical Fluids,* 34: 51–61.

Veriansyah B, Kim J D, Lee J C, Hong D, 2006a. Hydrothermal decomposition rate of thiodiglycol in supercritical water. *Journal of Industrial and Engineering Chemistry*, 12(3): 395–400.

Veriansyah B, Kim J D, Lee J C, Hong D, 2006b. Destruction of OPA from munitions demilitarization in supercritical water oxidation: kinetics of total organic carbon disappearance. *Journal of Environmental Science and Health: Part A*, 41: 1559–1568.

Veriansyah B, Kim J D, Lee J C, 2007. Destruction of chemical agents simulants in a supercritical water oxidation bench-scale reactor. *Journal of Hazardous Materials*, 147: 8–14.

Veriansyah B, Kim J D, Lee J C, 2009. A double wall reactor for supercritical water oxidation: Experimental results on corrosive sulfur mustard stimulant oxidation. *Journal of Industrial and Engineering Chemistry*, 15: 153–156.

Wagner W, Pruβ A, 2002. The IAWPS formulation 1995 for the thermodynamic properties of ordinary water substance for general and scientific use. *Journal of Physical and Chemical Reference Data,* 31(2): 387–535.